S. Nadeem*, Z. Ahmed and S. Saleem

The Effect of Variable Viscosities on Micropolar Flow of Two Nanofluids

DOI 10.1515/zna-2015-0491
Received November 22, 2015; accepted September 20, 2016; previously published online November 18, 2016

Abstract: A study of nanofluids is carried out that reveals the effect of rotational inertia and other physical parameters on the heat transfer and fluid flow. Temperature-dependent dynamic viscosity makes the microrotation viscosity parameter and the micro inertia density variant as well. The governing nonlinear partial differential equations are converted into a set of nonlinear ordinary differential equations by introducing suitable similarity transformations. These reduced nonlinear differential equations are then solved numerically by Keller-box method. The obtained numerical and graphical result discloses many interesting behaviour of nanofluids. It is seen that the temperature gradient decreases with the increase in viscosity parameter. Also, it is observed that with the fixed values of micropolar parameter and viscosity parameter, the velocity gradient near the wall increases with increasing values of solid particle volume fraction parameter. A suitable comparison of results is also presented in this study.

Keywords: Boundary Layer Flow; Nanofluid; Microrotation; Variable Viscosity.

1 Introduction

Nanofluids have attained significant attention in recent years owing to its wide range of applications in industrial as well as socioeconomic domain such as automotive industry, medical arena, nuclear power plant cooling system, and electronic cooling systems. Nanofluids are proved to be capable to handle some of the very important problems of emerged industrial growth; most significant among which is the problem to enhance the heat transfer ability of fluids and thermal management. The idea of nanofluids was first given by Choi [1] in 2001. Nanotechnology is now expected to play its role nearly in each and every industry. One of the main reasons for nanofluids wide spread implications is that its effective physical and thermophysical properties are adjustable according to need. Many authors have presented different kind of nanofluids for various flow geometries. Nadeem et al. [2] discussed the inspiration of induced magnetic field on a blood flow of Prandtl nanofluid model with stenosis. Dib et al. [3] presented approximate analytical solution of squeezing unsteady nanofluid flow. Vajravelu et al. [4] proposed the effect of variable viscosity on the flow and heat transfer of a viscous Ag–water and Cu–water nanofluids. Saleem et al. [5] explored the buoyancy and metallic particle effects on an unsteady water-based fluid flow along a vertically rotating cone. Sadiq et al. [6] deliberated the phenomena of partial slip effects on a rotating flow of two phase nanofluid over a stretching surface. Effect of thermal radiation on magneto hydrodynamics nanofluid flow and heat transfer by means of two phase model was studied by Sheikholeslami et al. [7]. Doganay and Turgut [8] reported enhanced effectiveness of nanofluid-based natural circulation mini loop. Experimental and numerical study of natural convection in a square enclosure filled with nanofluid was investigated by Hu et al. [9]. Zhang et al. [10] have performed experimental study of TiO2–water nanofluid flow and heat transfer characteristics in a multiport minichannel flat tube. Bi et al. [11] studied heat transfer characteristics and CHF prediction in nanofluid boiling. Abad et al. [12] examined experimental studies on the heat transfer and pressure drop characteristics of Cu–water and Al–water nanofluids in a spiral coil. An experimental study on the effect of Cu-synthesised/EG nanofluid on the efficiency of flat-plate solar collectors was deliberated by Zamzamian et al. [13]. Sulochana and Sandeep [14] presented dual solutions for radiative MHD forced convective flow of a nanofluid over a slandering stretching sheet in porous medium. Turkyilmazoglu [15] studied a note on the correspondence between certain nanofluid flows and standard fluid flows.

The geometry, deformation, and intrinsic motion such as rotation and spin motion of individual fluid element may affect the motion of the fluid and its heat transfer characteristics. Classical Naiver Stokes model takes into account the fluid motion as a whole but it does not discuss the behaviour of individual fluid element when undergoes

***Corresponding author: S. Nadeem,** Department of Mathematics, Quaid-I-Azam University 45320, Islamabad 44000, Pakistan, Tel.: + 9251 90642182, E-mail: snqau@hotmail.com
Z. Ahmed: Department of Mathematics, Quaid-I-Azam University 45320, Islamabad 44000, Pakistan
S. Saleem: Department of Sciences and Humanities, National University of computers and emerging sciences, Lahore, Pakistan

with spin inertia and micro rotational inertia. The concept of micropolar fluid was first proposed by Eringin [16] that can explain these intrinsic behaviours at very best both theoretically and practically. Micropolar fluid model supports couple stress and body torque. Unlike the ordinary fluid models, micropolar fluid model possesses the asymmetric stress tensor [17]. Hussain et al. [18] investigated radiation effects on the thermal boundary layer flow of a micropolar fluid towards a permeable stretching sheet. A note on micropolar fluid flow and heat transfer over a porous shrinking sheet was analysed by Turkyilmazoglu [19]. Rosca and Pop [20] have carried out the theoretical study of boundary layer flow past a permeable shrinking sheet in a micropolar fluid with a second-order slip flow model. Jayachandra et al. [21] have studied stagnation point flow of a micropolar fluid over a nonlinear stretching surface with suction. Sandeep and Sulochana [22] presented dual solutions for unsteady mixed convection flow of MHD micropolar fluid over a stretching/shrinking sheet with nonuniform heat source/sink. Micropolar fluid theory is developed to be a generalised case of Naiver Stokes model, In fact, the microrotation parameter that appears in the momentum equation shows the deviation of micropolar fluid model from that of classical Naiver Stokes model. Due to its tremendous applications and uses, many researchers have examined various aspects of this useful theory. Some are quoted in the studies [23–28].

In this study, micropolar fluid theory is incorporated on nanofluids. The fluid viscosities (dynamic viscosity, spin gradient viscosity, and micro-inertia density) are taken as inverse function of temperature. The flow is analysed with different values of physical and thermophysical parameters such as solid-particle volume fraction, viscosity parameter, and micro-inertia viscosity parameter. The effect of these parameters on the fluid flow and the heat transfer are determined numerically by Keller box method. The accuracy of the present results is also confirmed by comparing the results with the existing literature.

2 Mathematical Formulation

Consider a two-dimensional, steady, boundary layer laminar flow of a micropolar fluid over a semi-infinite impermeable flat surface. The flow takes place in the positive xy-plane with the surface being at $y=0$. The lower surface is fixed at constant temperature T_w, whereas the temperature of the fluid far away from the surface is taken to be T_∞. Fluid near the surface is at rest and attains free stream velocity U_∞ far away from the surface as shown in Figure 1.

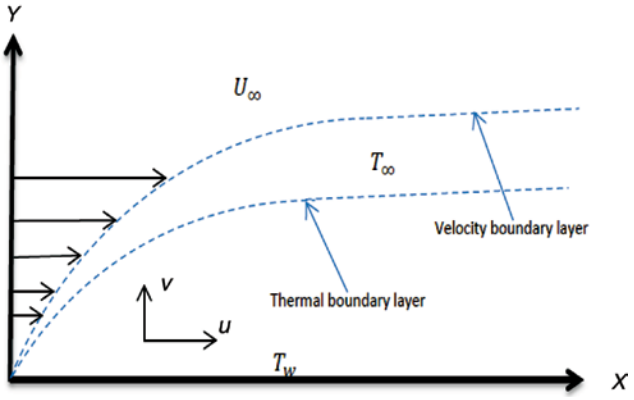

Figure 1: Schematic diagram of boundary layer flow.

The assumed fluid is water-based micropolar nanofluid with nano-solid particles of either copper (Cu) or silver (Ag). The working fluid is assumed to be incompressible, no-chemical reactions, negligible internal heat generation or absorption, and negligible radiative heat transfer. The viscosity of the nanofluid is considered to be variable and is taken as the inverse function of temperature. In the absence of viscous dissipation, the usual boundary layer approximation leads the governing equations of mass, momentum, angular momentum, and energy, respectively [4].

$$\frac{\partial u}{\partial x}+\frac{\partial v}{\partial y}=0, \tag{1}$$

$$u\frac{\partial u}{\partial x}+v\frac{\partial u}{\partial y}=\frac{1}{\rho_{nf}}\frac{\partial}{\partial y}(\mu_{nf}+\kappa)\frac{\partial u}{\partial y}+\frac{\kappa}{\rho_{nf}}\frac{\partial N}{\partial y}, \tag{2}$$

$$u\frac{\partial N}{\partial x}+v\frac{\partial N}{\partial y}=\frac{1}{(\rho_{nf})j}\frac{\partial}{\partial y}\left(\gamma^{*}\frac{\partial N}{\partial y}\right)-\frac{\kappa}{(\rho_{nf})j}\left(2N+\frac{\partial u}{\partial y}\right), \tag{3}$$

$$u\frac{\partial T}{\partial x}+v\frac{\partial T}{\partial y}=\alpha_{nf}\frac{\partial^2 T}{\partial y^2}, \tag{4}$$

The appropriate boundary conditions are

$$\begin{aligned}&u(x,y)=0,\ v(x,y)=0,\ T(x,y)=T_w,\ N=-N_0\frac{\partial u}{\partial y}\ \text{at}\ y=0,\\ &u(x,y)\to U_\infty,\ T(x,y)\to T_\infty,\ N\to 0\ \text{as}\ y\to\infty,\end{aligned} \tag{5}$$

where u and v are the fluid velocity components in the stream direction and cross stream direction, respectively, T is the temperature of the fluid, N is the microrotation or angular velocity of the fluid particle, and κ is the vortex viscosity or microrotation viscosity. The effective density of the nanofluid is [4] $(\rho)_{nf}=(1-\phi)\rho_{f\infty}+\phi\rho_s$, where ρ_s is the

density of the solid particles, ρ_{f_∞} is the density of the base fluid and ϕ denotes the volume fraction of the nano-solid particles in the fluid, μ_{nf} is the effective dynamic viscosity of the nanofluid which is given as [4] $\mu_{nf}=\frac{\mu_f}{(1-\phi)^{2.5}}$, here μ_f is the coefficient of dynamic viscosity which vary as an inverse function of temperature, i.e. $\frac{1}{\mu_f}=a(T-T_r)$. Since $a=\frac{\delta}{\mu_{f_\infty}}$, $T_r=T_\infty-\frac{1}{\delta}$, δ, and a are constants, and $a>0$ for liquids, γ^* is the spin gradient viscosity and is given as [24] $\gamma^*=\left(\mu_{nf}+\frac{\kappa}{2}\right)j$, where j is the micro-inertia density. The thermal diffusibility of the nanofluid is $\alpha_{nf}=\frac{K_{nf}}{(\rho C_p)_{nf}}$, in which K_{nf} is the thermal conductivity of the nanofluid which is given as [4] $K_{nf}=K_{f_\infty}\left[\frac{K_s+2K_{f_\infty}-2\phi(K_{f_\infty}-K_s)}{K_s+2K_{f_\infty}+\phi(K_{f_\infty}-K_s)}\right]$. The effective heat capacitance of the nanofluid can be written as $(\rho C_p)_{nf}=(1-\phi)(\rho C_p)_{f_\infty}+\phi(\rho C_p)_s$. The suffixes *nf*, f_∞, and *s* indicate the thermophysical properties of nanofluid, base fluid, and solid particles, respectively.

3 Similarity Transformations

Equations (1–4) are the nonlinear partial differential equations that are converted into a set of nonlinear ordinary differential equations by choosing a specific forms of the velocity, angular velocity, and temperature [4].

$$\eta=\left(\frac{U_\infty}{2\nu_\infty x}\right)^{\frac{1}{2}}y,\ \psi=(2\nu_\infty U_\infty x)^{\frac{1}{2}}f(\eta),\ \theta(\eta)=\frac{T-T_\infty}{T_w-T\infty},$$
$$N=U_\infty\left(\frac{U_\infty}{2\nu_\infty x}\right)^{\frac{1}{2}}g(\eta),\ u=\frac{\partial\psi}{\partial y},\ v=-\frac{\partial\psi}{\partial x},\ j=x^2\,\mathrm{Re}_x^{-1}f^2(\eta),\quad(6)$$

where η is the similarity variable, f, N, and θ are the dimensionless velocity, microrotation, and temperature, respectively. The velocity components automatically satisfy the continuity equation (1). Using the above similarity transformations, the governing equations (2–4) are reduced as

$$\frac{f'''}{\left(1-\frac{\theta}{\theta_r}\right)}+\frac{f''\theta'}{\theta_r\left(1-\frac{\theta}{\theta_r}\right)^2}+(1-\phi)^{2.5}\left[1-\phi+\phi\left(\frac{\rho_s}{\rho_{f_\infty}}\right)\right]ff''+K(1-\phi)^{2.5}f'''+K(1-\phi)^{2.5}g'=0,\quad(7)$$

$$\frac{f^2g''}{\left(1-\frac{\theta}{\theta_r}\right)}+(1-\phi)^{2.5}\left[\frac{K}{2}f^2g''-K(f''+2g)+Kff'g'+\left[1-\phi+\phi\left(\frac{\rho_s}{\rho_{f_\infty}}\right)\right](f^2f'g+f^3g')\right]+\frac{2ff'g'}{\left(1-\frac{\theta}{\theta_r}\right)}+\frac{f^2g'\theta'}{\theta_r\left(1-\frac{\theta}{\theta_r}\right)^2}=0,\quad(8)$$

$$\theta''+\mathrm{Pr}\frac{K_{f_\infty}}{K_{nf}}\left[1-\phi+\phi\frac{(\rho C_p)_s}{(\rho C_p)_{f_\infty}}\right]f\theta'=0,\quad(9)$$

The boundary conditions in transformed form reduce to

$$\begin{aligned}&f(\eta)=0,\ \theta(\eta)=1,\ g(\eta)=-N_0f''(\eta),\ f'(\eta)=0\ \text{at}\ \eta=0\\&f'(\eta)\to1,\ \theta(\eta)\to0,\ g(\eta)\to0\ \text{as}\ \eta\to\infty.\end{aligned}\quad(10)$$

Here $K=\frac{\kappa}{\mu_{f_\infty}}$ is the micropolar parameter, $\theta_r=-\frac{1}{\delta(T_w-T_\infty)}$ is the fluid viscosity parameter, and $\mathrm{Pr}=\frac{\nu_{f_\infty}}{\alpha_{f_\infty}}$ represents the Prandtl number of the base fluid. The skin friction coefficient and the Nusselt number for the flow problem are given as

$$C_f=\frac{1}{(1-\phi)^{2.5}}\left(1-\frac{1}{\theta_r}\right)^{-1}(\mathrm{Re}_x)^{-\frac{1}{2}}f''(0),\quad(11)$$

$$\mathrm{Nu}_x=-(\mathrm{Re}_x)^{\frac{1}{2}}\frac{K_{nf}}{K_{f_\infty}}\theta'(0).\quad(12)$$

Where $\mathrm{Re}_x=U_\infty x/\nu_{f_\infty}$ is the local Reynolds number.

4 Solution Methodology

The transformed nonlinear ordinary differential equations are then solved by an implicit finite difference scheme known as Keller box method [29]. This scheme consists of finite difference method, Newton's method and block elimination technique. It is an implicit scheme with second order accuracy and is unconditionally stable.

Keller box scheme is much faster, more efficient, and flexible to apply on nonlinear boundary value problems. This scheme works effectively on the problem having complex physical situations and can be easily

implemented to accommodate the variable physical and thermophysical properties of the fluid. The numerical solutions are obtained in four steps. At the very first, the system of ordinary differential equations are converted into the system of first-order ordinary differential equations that are then secondly, discritise by using central difference scheme. In the third step, the discretised equations are linearised by applying Newton's linearisation method and write the equations into vector matrix form. At very last infact the fourth step, the linearised system of equations are solved by block elimination technique. This last step is done with the help of Matlab programming. Matlab 7.9 version is used for the algorithm. $\Delta\eta = 0.01$, step size is taken for all of the computations. Error tolerance is fixed at 10^{-6} for all of the calculations. The edge of the boundary layer is fixed at $\eta_\infty = 10$, which is sufficient to attain the far field boundary conditions asymptotically for all values of the parameters considered here. The obtained results are authenticated by comparing the results of simplest case with another numerical technique. Temperature gradient and velocity gradient near the wall is calculated with different values of parameters for the case when micropolar parameter vanishes. This is done with the help of Maple software. A finite difference method which is called midrich method is incorporated for this matter. Continuation approach is implemented to solve the problem. The results are in very good agreement with the solutions obtained by Keller box method. Details on the convergence and stability of the methods can be found in detail in following articles [29–31].

Table 1: Thermophysical properties of base fluid and nanoparticles [4].

	Base fluid	Cu-nanoparticles	Ag-nanoparticles
C_p (J/kgK)	4179	385.0	235.0
ρ (kg/m^3)	997.1	8933.0	10500
k (w/mK)	0.613	400.0	429.0
α (10^{-7}m^2/s)	1.470	1163.1	1738.6

5 Numerical Results

Thermophysical properties are assumed to be constant except the dynamic viscosity that makes the microrotation viscosity and micro-inertia density variant as well.

These readings are obtained with respect to different values of various parameters that are nanoparticle volume fraction, microrotation parameter, and dynamic viscosity parameter.

6 Graphical Results and Discussions

Numerical as well as graphical results are obtained to study the impact of different physical properties of nanofluid on the flow and heat transfer phenomena. Most importantly, the effect of viscosity parameter "θ_r" on the flow and heat transfer is discussed in the presence of rotational inertia.

Table 1 represents standard values of thermophysical properties which are used throughout the computations. Tables 2 and 3 are presented to verify the stability of present results in the absence of microrotation parameter with the published results [4] for Ag–water and Cu–water nanofluid, respectively. The results are seen to be in decent compatible order with each other. Numerical results of velocity gradient and wall temperature gradient are mentioned in Tables 4–7 with Cu–water and Ag–water nanofluid, respectively, in the presence of microrotation parameter. The obtained results uncover some very interesting facts. Some

Table 2: Comparison of present findings with those of Vajravelu [4] with Ag–water nanofluid in the absence of K.

	ϕ	Midrich method		Keller box method		Published results [4]
		$f''(0)$	$\theta'(0)$	$f''(0)$	$\theta'(0)$	$\theta'(0)$
	0.0	0.550369	−0.928805	0.550330	−0.928881	−0.928881
$\theta_r = -5$	0.1	0.668561	−0.885582	0.668640	−0.885595	−0.885574
	0.20	0.700164	−0.807416	0.700496	−0.807441	−0.807498
	0.0	0.510522	−0.912024	0.510940	−0.912538	−0.912522
$\theta_r = -10$	0.10	0.622749	−0.871297	0.622709	−0.871208	−0.871263
	0.20	0.653878	−0.795190	0.653084	−0.795127	−0.795198
	0.0	0.470015	−0.895041	0.470056	−0.895064	−0.895025
$\theta_r \to \infty$	0.10	0.575775	−0.855873	0.575762	−0.855832	−0.855851
	0.20	0.606176	−0.781814	0.606312	−0.781870	−0.781897

Table 3: Comparison of present findings with those of Vajravelu [4] with Cu–water nanofluid in the absence of K.

	ϕ	Midrich method		Keller box method		Published results [4]
		$f''(0)$	$\theta'(0)$	$f''(0)$	$\theta'(0)$	$\theta'(0)$
	0.0	0.550369	−0.928826	0.550930	−0.928820	−0.928881
$\theta_r = -5$	0.1	0.668561	−0.881215	0.669642	−0.881268	−0.881500
	0.20	0.700164	−0.807501	0.701416	−0.807593	−0.807557
	0.0	0.510522	−0.912285	0.510980	−0.912227	−0.912522
$\theta_r = -10$	0.10	0.622749	−0.867058	0.623709	−0.867006	−0.867051
	0.20	0.653878	−0.794547	0.655016	−0.794594	−0.794952
	0.0	0.470015	−0.895915	0.470376	−0.895937	−0.895025
$\theta_r \to \infty$	0.10	0.575775	−0.851280	0.576618	−0.851218	−0.851507
	0.20	0.606176	−0.781340	0.607201	−0.781325	−0.781345

Table 4: Numerical results for wall velocity gradient against various values of pertinent parameters Cu–water micropolar nanofluid.

	ϕ	$K=0.5$ $f''(0)$	$K=1$ $f''(0)$	$K=2$ $f''(0)$
	0.0	0.483388	0.454148	0.502364
$\theta_r = -5$	0.1	0.588668	0.567407	0.668297
	0.20	0.626931	0.614291	0.753158
	0.0	0.461378	0.437371	0.435353
$\theta_r = -10$	0.10	0.560405	0.546223	0.576318
	0.20	0.594623	0.589104	0.710869
	0.0	0.436941	0.419082	0.418816
$\theta_r \to \infty$	0.10	0.529283	0.522139	0.553600
	0.20	0.559778	0.579887	0.620296

Table 5: Numerical results for wall temperature gradient against various values of pertinent parameters with Cu–water micropolar nanofluid.

	ϕ	$K=0.5$ $\theta'(0)$	$K=1$ $\theta'(0)$	$K=2$ $\theta'(0)$
	0.0	−0.962254	−0.994366	−1.233808
$\theta_r = -5$	0.1	−0.901948	−0.916842	−1.149227
	0.20	−0.818569	−0.831001	−1.009486
	0.0	−0.942205	−0.967182	−1.066112
$\theta_r = -10$	0.10	−0.884556	−0.903435	−0.999765
	0.20	−0.805721	−0.814254	−0.947964
	0.0	−0.923294	−0.946490	−1.041574
$\theta_r \to \infty$	0.10	−0.870297	−0.886186	−0.979681
	0.20	−0.793493	−0.832353	−0.874869

Table 6: Numerical results for wall velocity gradient against various values of pertinent parameters with Ag–water micropolar nanofluid.

	ϕ	$K=0.5$ $f''(0)$	$K=1$ $f''(0)$	$K=2$ $f''(0)$
	0.0	0.483388	0.457119	0.522138
$\theta_r = -5$	0.1	0.615241	0.631147	0.724400
	0.20	0.665781	0.706388	0.844302
	0.0	0.461378	0.437371	0.435353
$\theta_r = -10$	0.10	0.585997	0.572765	0.610198
	0.20	0.631937	0.638123	0.781573
	0.0	0.436941	0.421252	0.435955
$\theta_r \to \infty$	0.10	0.558655	0.554331	0.609113
	0.20	0.601993	0.644665	0.706979

Table 7: Numerical results for wall temperature gradient against various values of pertinent parameters with Ag–water micropolar nanofluid.

	ϕ	$K=0.5$ $\theta'(0)$	$K=1$ $\theta'(0)$	$K=2$ $\theta'(0)$
	0.0	−0.962254	−1.011872	−1.260144
$\theta_r = -5$	0.1	−0.905901	−0.985668	−1.158294
	0.20	−0.818238	−0.894400	−1.0137132
	0.0	−0.942205	−0.967182	−1.066112
$\theta_r = -10$	0.10	−0.888463	−0.907880	−1.008217
	0.20	−0.806141	−0.826862	−0.989569
	0.0	−0.923294	−0.963965	−1.090451
$\theta_r \to \infty$	0.10	−0.887393	−0.906089	−1.042381
	0.20	−0.803495	−0.863685	−0.923841

of these observations are discussed meticulously with valid arguments. It is observed that the general behaviour of Ag–water and Cu–water nanofluids are all same. It is very clear from the obtained data that with the fixed values of micropolar parameter and viscosity parameter the velocity gradient near the wall increases with increasing values of solid particle volume fraction parameter, this behaviour of nanofluid causes the skin friction to rise and in result the momentum decreases which brings thinning effect in the momentum boundary layer.

On the other hand, the numerics depicts that for each fixed value of micropolar parameter and viscosity parameter the magnitude of wall temperature gradient decreases with increasing values of solid particle volume

fraction, since with the decrease in the wall temperature gradient the heat flux from the solid boundaries to the fluid body decreases which causes the thinning of thermal boundary layer thickness. It is because with the low-temperature potential between the two ends the thermal boundary layer is nearer to achieve. It can be noted from the numerical tables that for nanofluids with rotational inertia the magnitude of temperature gradient decreases with the increase in the magnitude of viscosity parameter, whereas the wall velocity gradient decreases as well. Since the decrease in the wall velocity gradient indicates the decrease in the skin friction, it can be concluded that momentum boundary layer thickness increases with the increase in the magnitude of viscosity parameter. It is very obvious for heat flux since increasing viscosity parameter represents the decreasing difference of wall temperature and the temperature outside the thermal boundary layer, which of course results in the fall of heat flux.

The obtained numerical results both for Ag–water and Cu–water nanofluids clearly show that with the rise in microrotation parameter the Nusselt number increases and hence heat flux increases which causing the thickening effect on thermal boundary layer. Figures 2–5 presents the velocity profile with different parameters. It is observed that velocity is zero near the wall; it increases and tends to unity as the distance increases from the solid boundaries. Figure 2 depicts the variation of velocity profile for various values of microrotation parameter. It is obvious from the figure that the magnitude of velocity is greater in the presence of solid particle volume fraction parameter. Figure 3 shows that in the presence of rotational inertia

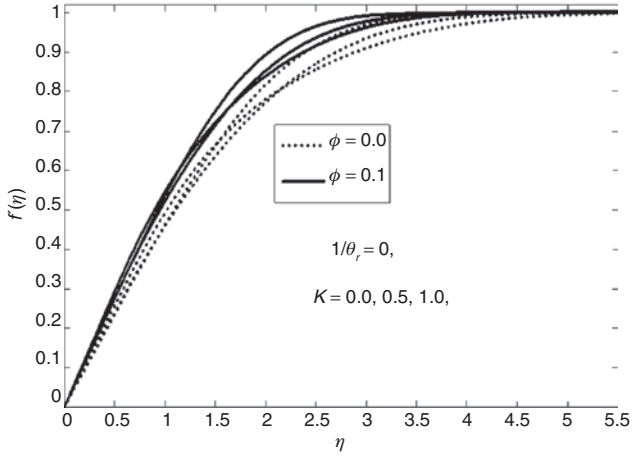

Figure 2: Effects of K and ϕ on velocity $f'(\eta)$, when $\theta_r \to \infty$ for Ag–water.

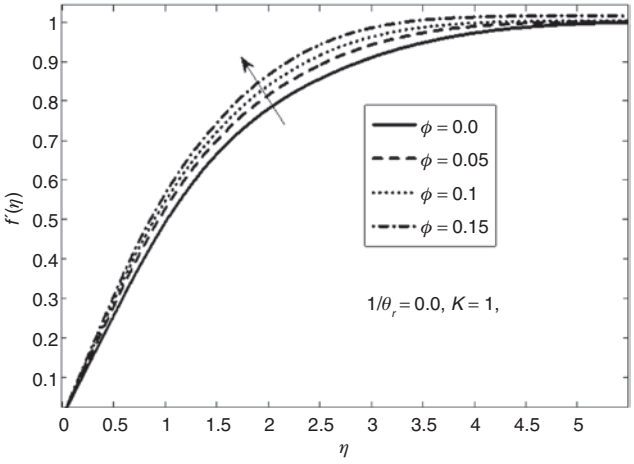

Figure 3: Effects of ϕ on velocity $f'(\eta)$, when $\theta_r \to \infty$ for Ag–water.

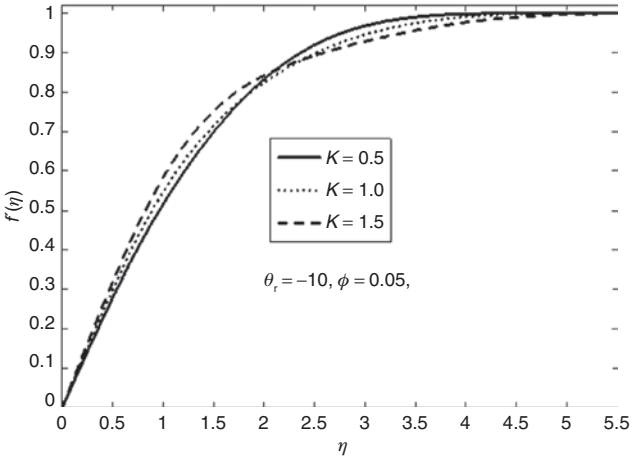

Figure 4: Effects of K on velocity $f'(\eta)$, for $\theta_r \to 0$ for Ag–water.

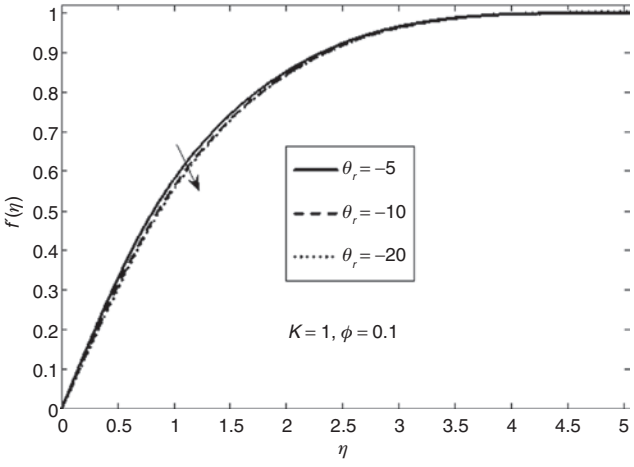

Figure 5: Effects of θ_r on velocity $f'(\eta)$ for Ag–water.

the velocity profile increases with increasing value of solid particle volume fraction parameter. The profiles of velocity increase in the region $0 \le \eta \le 2$ and decrease in the region $2 \le \eta \le 5.5$ for increasing values of microrotation parameter (see Figure 4). Figure 5 shows the decrease in velocity distribution with the increase in the magnitude of viscosity parameter.

Figures 6–9 shows the temperature profile in the presence of rotational inertia and other different physical parameters. It is observed that the temperature distribution starts from unity near the wall and tends to vanish as the distance increases from the solid boundaries. Figure 6 indicates the increase in temperature distribution with the increase in the magnitude of viscosity parameter. It is because as the temperature distribution increases the heat flux decreases which results in the decrease in thermal potential difference between the two ends of fluid body, this is very obvious since viscosity parameter is reciprocal of this temperature difference. Figure 7 shows the increase in the temperature distribution with the rise in the volume fraction parameter. It is so because the rise in the volume fraction of solid particles increase the thermal conductivity of the nanofluid and hence increases the temperature distribution. It is very clear from the Figure 8 that the temperature profile decreases with the increasing values of micropolar parameter, the behaviour is even true when viscosity is taken as function of temperature as shown in Figure 9. Figures 10 and 11 show that the variation of velocity is greater than for Ag–water, but temperature of the fluid does not show much variation, respectively.

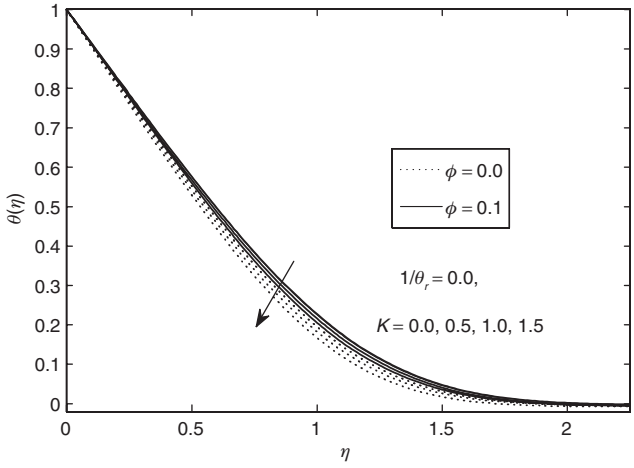

Figure 8: Effects of ϕ and K on temperature $\theta(\eta)$, for $\theta_r \to \infty$ for Ag–water.

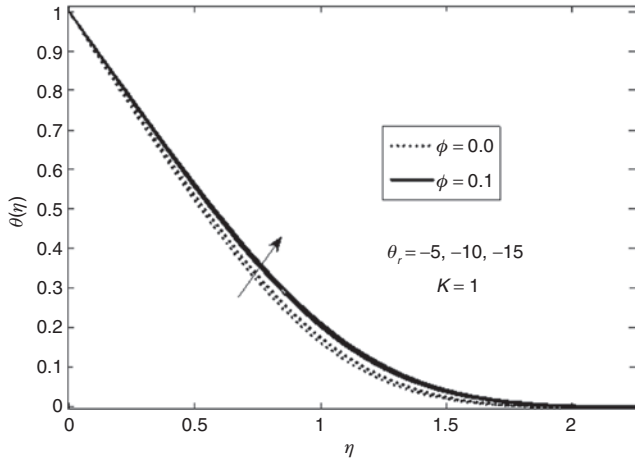

Figure 6: Effects of ϕ and θ_r on temperature $\theta(\eta)$ for Ag–water.

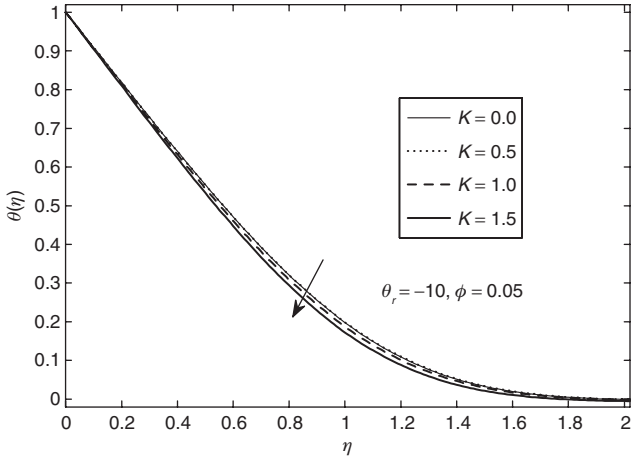

Figure 9: Effects of K on temperature $\theta(\eta)$, for $\theta_r < 0$ for Ag–water.

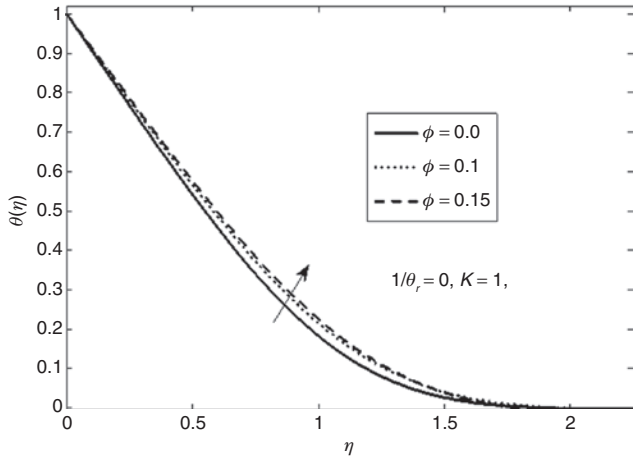

Figure 7: Effects of ϕ on temperature $\theta(\eta)$, for $\theta_r \to \infty$ for Ag–water.

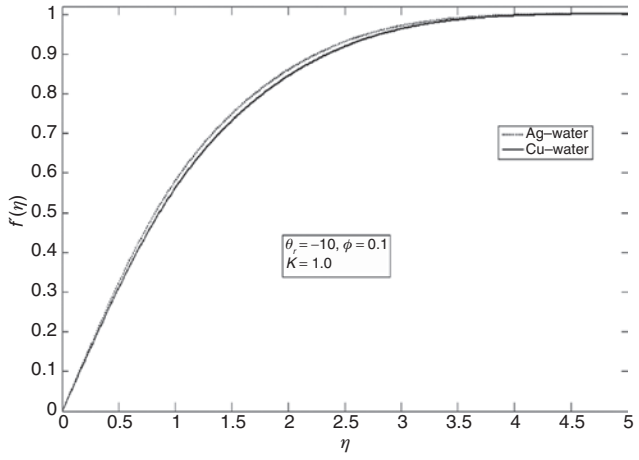

Figure 10: Comparison of Cu–water and Ag–water for velocity.

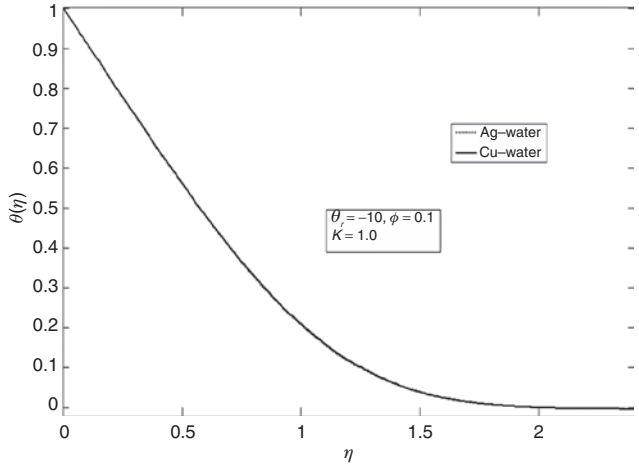

Figure 11: Comparison of Cu–water and Ag–water for temperature.

7 Conclusion

Numerical study of micropolar nanofluids has uncover very interesting facts about the fluid flow and heat transfer phenomena in the presence of temperature-dependent viscosities. The above-mentioned study can be concluded into two important observations. Since dynamic viscosity is the inverse function of temperature, therefore the rise in the temperature difference fasten the fluid flow. Secondly, the increase in rotation parameter is simultaneous to the raise in the heat flux through the system. Further both velocity and temperature are an increasing functions of volume fraction parameter. Moreover temperature profile reduces with the micropolar parameter. It is also found that the presence of rotational inertia, velocity profile increases with increasing value of solid particle volume fraction parameter. The variation of velocity is greater than for Ag–water, but temperature of the fluid does not show much variation. The results attained for the flow and heat transfer characteristics reveal various interesting behaviours that warrant further study of nanofluids.

Nomenclature

u, v	fluid velocities along stream direction and cross stream direction, respectively
T, N	temperature and angular velocity of the fluid
f, θ	dimensionless velocity and temperature, respectively
T_w, T_∞	temperature of the fluid near and far away from the surface
U_∞, g	free stream velocity, dimensionless angular velocity, respectively
ρ_{nf}, μ_{nf}	effective density and viscosity of nanofluid
ρ_{nf}, μ_{nf}	effective density and viscosity of nanofluid
α_{nf}, K_{nf}	Thermal diffusibility and effective thermal conductivity of the nanofluid
ϕ	volume fraction of the nano solid particles
θ_r, γ^*	viscosity parameter, spin gradient viscosity, respectively
κ, j	vertex viscosity, micro inertia density, respectively
C_p, Pr	heat capacitance, Prandtl number, respectively
C_f, Nu_x	skin friction coefficient, Nusselt number, respectively
Re_x, K	local Reynold,s number, micropolar parameter

References

[1] S. U. S. Choi, Z. G. Zhang, and W. Yu, App. Phy. Lett **79,** 2252 (2001).
[2] S. Nadeem, S. Ijaz, and M. A. Sadiq, Curr. Nanosci. **10,** 753 (2014).
[3] A. Dib, A. Haiahem, and B. Bou-said, Powder Tech. **269,** 193 (2015).
[4] V. Kuppalapalle, P. K. Vinayaka, and N. G. Chiu-On, J. Hydrodynamics **25,** 1 (2013).
[5] S. Saleem, S. Nadeem, and R. Ul Haq, Eur. Phys. J. Plus **129,** 213 (2014).
[6] M. A. Sadiq, S. Nadeem, A. U. Rehman, and R. Mehmood, Curr. Nanosci. **10,** 846 (2014).
[7] M. Sheikholeslami, D. D. Ganji, M. Y. Javed, and R. Ellahi, J. Magn. Magn. Mater. **374,** 36 (2015).
[8] S. Doganay and A. Turgut, App. Thermal Eng. **75,** 669 (2015).
[9] Y. Hu, Y. He, Cong Qi, B. Jiang, and H. Inaki Schlaberg, Int. J. Heat Mass Transf. **78,** 380 (2014).
[10] J. Zhang, Y. Diao, Y. Zhao, and Y. Zhang, Int. J. Heat Mass Transf. **79,** 628 (2014).
[11] J. Bi, K. Vafai and D. M. Christopher, Int. J. Heat Mass Transf. **80,** 256 (2015).
[12] M. T. Jamal-Abad, A. Zamzamian, and M. Dehghan, Exp. Therm. Fluid Sci. **47,** 206 (2013).
[13] A. Zamzamian, M. KeyanpourRad, M. Kiani Neyestani, M. T. Jamal-Abad, Renew. Energy **71,** 658 (2014).
[14] C. Sulochana and N. Sandeep, J. Naval Architecture Marine Eng. **12,** 115 (2015).
[15] M. Turkyilmazoglu, J. Heat Transf. **137,** 024501 (2015).

[16] A. C. Eringen, J. Math. Mech. **16,** 18 (1966).
[17] G. Lukaszewicz. Micropolar Fluids Theory and Applications, Springer 1999.
[18] M. Hussain, M. Ashraf, S. Nadeem, M. Khan, J. Franklin Inst. **350,** 194 (2013).
[19] M. Turkyilmazoglu, Int. J. Heat Mass Transfer **72,** 388 (2014).
[20] N. C. Rosca, I. Pop, Eur. J. Mech. B Fluids **48,** 115 (2014).
[21] M. Jayachandra Babu, C. S. K. Raju, and N. Sandeep, Int. J. Sci. c Eng. Research **9,** 67 (2015).
[22] N. Sandeep and C. Sulochana, Eng. Sci. Tech., Int. J. **18,** 738 (2015).
[23] A. Borrelli, G. Giantesio, and M. C. Patria, Int. J. Heat Mass Transf. **80,** 614 (2015).
[24] M. Jayachandra Babu, R. Gupta, and N. Sandeep, J. Basic Appl. Res. Int. **7,** 73 (2015).
[25] G. C. Bourantas and V. C. Loukopoulos, Int. J. Heat Mass Transf. **79,** 930 (2014).
[26] D. A. S Rees and A. P. Bassom, Int. J. Eng. **34,** 113 (1996).
[27] M. Turkyilmazoglu, Int. J. Nonlinear Mech. **83,** 59 (2016).
[28] M. S. Faltas and E. I. Saad, Eur. J. Mech. B Fluids **48,** 266 (2014).
[29] H. B. Keller, Numerical Methods for Two-point Boundary Value Problems. New York, USA, Dover 1992.
[30] P. C. Meek and O. Norbury, Siamj. Numer. Anal **5,** 21 (1984).
[31] K. Vajravelu, K. V. Prasad, Keller – Box Method and Its Application, Chapter 3. Applied Numerical Analysis, Fifth edition, Addison-Wesley Publishing Company, New Jersey 1994.